HEFAT2014
10th International Conference on Heat Transfer, Fluid Mechanics and Thermodynamics
14 – 16 July 2014
Orlando, Florida

TRANSIENT NATURAL CONVECTION FLOW DYNAMICS IN A ASYMMETRICALLY HEATED VERTICAL CHANNEL

G. Polidori[1], S. Fatnassi[2], R. Ben Maad[2], F. Beaumont[1], S. Fohanno[1,*]
*Author for correspondence
[1] Groupe de Recherche en Sciences Pour l'Ingénieur (GRESPI EA4694),
University of Reims Champagne-Ardenne,
BP1039, 51687 Reims,
France,
E-mail: stephane.fohanno@univ-reims.fr

[2] Laboratoire d'Energétique et des Transferts Thermique et Massique (LETTM),
University of Tunis El Manar,
Tunis,
Tunisia,

ABSTRACT

An experimental study in an open-ended vertical channel is carried out in order to describe the fluid dynamics during the early stage regime of free convection inside a vertical channel asymmetrically heated at uniform heat flux. The flow dynamics were characterized both by means of flow visualization techniques based on laser tomography and by velocity field measurements in the plane of symmetry of the channel using 2D-PIV (Particle Image Velocimetry) technique. The analysis allowed to detect a complex topological behaviour in the internal flow leading to numerous instabilities whose topological features are described. Vortex formation and shedding, vortex splitting, separation and beating of the boundary layer from one wall to another are identified, leading to an imbalance in the outlet pressure field which is certainly at the origin of a large-scale reversal flow.

INTRODUCTION

This experimental work is part of a series of studies conducted by the French Research Group GDR AMETh (*Analyse – Maîtrise des écoulements et Echanges Thermiques*) on natural convection in open-ended channels. The main objective of these studies is to allow a better prediction of the thermal and dynamic behaviour of free-convective flows in open-ended channels by developing reliable numerical simulation tools [1]. The validation step of these tools requires the establishment of experimental setups for providing the necessary thermal and dynamic data [2]. The present work aims at providing such data by experimentally investigating the flow dynamics in a vertical channel heated asymmetrically.

The heated vertical open-ended channel is representative of several problems of practical interest such as the chimney, the solar panel or the Trombe wall [3-5]. Natural convection in open-ended vertical channels has been widely studied, both experimentally and numerically, since the pioneering work of Elenbaas [6]. For many years, experimental studies carried out on natural convection in vertical open-ended channels were mainly concerned with thermal measurements (flow and wall temperature) both for uniform heat flux (UHF) and for uniform wall temperature (UWT) problems [5-9]. The natural convection flow dynamics in parallel-plate channels has also been investigated by means of flow visualization techniques [2,7,10], Laser Doppler Velocimetry [10-15] and more recently by Particle Image Velocimetry [16]. Sparrow et al. [17] performed flow visualizations in an asymmetrically heated water channel. They observed a flow reversal close to the unheated wall. Ospir et al. [2] investigated the influence of the channel aspect ratio and the Rayleigh number on the flow structure, also in the case of asymmetric heating. A recent work by Dupont et al. [10] stressed the need to generalize the conditions of existence of the reverse flow by quantifying its global characteristics and extend the range of tested parameters, namely the Rayleigh number and the aspect ratio.

In parallel, several numerical studies have been carried out [1,18,19] in an attempt to predict the heat transfer and flow field characteristics in open channels. However, despite these efforts, the prediction remains an open problem. At the level of knowledge and current thinking, it seems clear that numerical simulations of free convection in open domain require further developments before being usable for design. This can only be possible by the contribution of new experiments necessary to

understand physical phenomena that drive the flow behaviour, to generate reference measurements, to validate numerical simulations in order to find out reliable ways to enhance heat transfer.

In order to reach this goal, the study presented in this paper focused more specifically on the very first moments of the implementation of this channel flow, with the assumption that the flow reversal phenomena, poorly understood to date, find their explanation in the history of their appearance. The flow dynamics were characterized both by means of flow visualization techniques based on laser tomography and by velocity field measurements in the plane of symmetry of the channel using 2D-PIV (Particle Image Velocimetry) technique. To the authors' knowledge, it is the first time that such a study focuses on the early stages in the development of reversal flows in open-ended channels.

NOMENCLATURE

A	[m]	Heated length
b	[m]	Channel wall spacing
d	[m]	Diameter
g	[m/s²]	Acceleration of gravity
Gr	[-]	Grashof number based on wall heat flux and channel wall spacing ($=\frac{g\beta\varphi_w b^4}{k\nu^2}$)
k	[W/mK]	Thermal conductivity
L	[m]	Recirculation length
Pr	[-]	Prandtl number
Ra	[-]	Rayleigh number based on heat flux and channel wall spacing (=Gr.Pr)
Ra^*	[-]	Modified Rayleigh number (=Ra/R_f)
R_f	[-]	Aspect ratio (=A/b)
t	[s]	Time
T	[K]	Temperature
v	[m/s]	Vertical velocity component
V_S	[m/s]	Sedimentation velocity
x	[m]	Horizontal coordinate
y	[m]	Vertical coordinate

Special characters

β	[1/K]	Volume expansion coefficient
δ	[m]	Hydrodynamical boundary layer thickness
δ_T	[m]	Thermal boundary layer thickness
Δ	[-]	Thermal to hydrodynamical boundary layer thickness ratio ($=\delta_T/\delta$)
ρ	[kg/m³]	Density
ν	[m²/s]	Kinematic viscosity
φ	[W/m²]	Heat flux

Subscripts

f	Fluid
p	Particle
w	Wall
∞	Ambient

EXPERIMENTAL FACILITIES

The channel geometry

Experimental investigations of the dynamics of the natural convection flow have been carried out in a vertical plane channel heated asymmetrically [2]. The channel is located in a vertical tank filled with water. The choice of water as working fluid leads to a negligible effect of heat transfer by radiation to only focus on free convection effects. The channel is composed of two vertical parallel plane walls separated by an adjustable distance (b). In the present study, the width b was fixed at $36\,\text{mm}$. One wall is composed of a heated central part (height $A = 188\,\text{mm}$) and two unheated extensions (height A/2) respectively located at the bottom and top open-ends of the channel while the opposite wall remains entirely unheated throughout the duration of the experiments (Figure 1). The heating of the central half part of the heated wall is provided by a fabric heater which delivers a heat flux uniformly distributed throughout the heating zone. This thermal system (Figure 1) consists of a vertical plane thermofoil heater, covered by a 3 mm-thick aluminum plate on the channel side, delivering an adjustable heat flux φ_w to water in the channel.

PIV System

The experimental device is set in a tank filled with water (15°C) and seeded with hollow glass spheres (8 µm ≤ diameter ≤ 12 µm). The experimental configuration of the PIV measurement system [20] includes a LITRON Nd: YAG laser emitting at 532 nm with a maximum power of $135\,\text{mJ}$. The laser sheet is created throughout a cylindrical lens. Image acquisition is done by a CCD camera, Flow sense model, which is able to record 14-bit black and white images. The duration of a laser pulse is 250 ms and the acquisition frequency is 4 Hz.

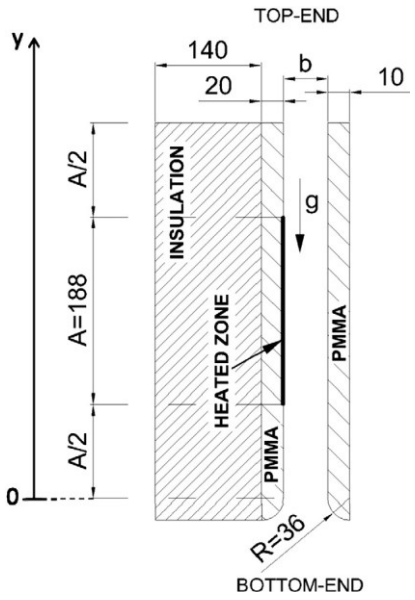

Figure 1 Edge view of the vertical open channel

Due to the fairly low velocities of the liquid phase, image acquisition is performed in single frame mode by a sequence of 6 images. The doublets are reconstructed from all the images acquired in single frame mode. The averaged correlation is used as analysis method. This method can reproduce a vector field from several pairs of images by determining the average correlation in an interrogation zone. Derived parameters such as vorticity fields, streamline patterns can be deduced from the initial velocity maps.

Heat flux evaluation

One of the main difficulties of this kind of experiments conducted with the use of heated walls (in channel configuration or not) is the exact evaluation of the value of the heat source which is the flow engine, by estimating in a fine way the precise part of the heat flux which is convected within the fluid. Similar procedure to calculate the heat flux delivered to water had been previously used in an experimental study of transient free convection flow on a vertical heated surface with an array of ribs [21]. The wall heat flux distribution was checked by means of temperature measurements along the heated plate. For this check, a configuration of natural convection boundary layer flow along a vertical flat plate immersed in a semi-infinite fluid medium was selected. This flow configuration was obtained by simply removing the cold wall of the channel from the experimental setup. Wall surface temperature measurements were carried out along the heated vertical plate. For this purpose, nine chromel–alumel type thermocouples were vertically stuck on the water side of the vertical heated wall (188 mm height) and a special attention had been paid to the surface gluing process in order to avoid the insertion of a thermal resistance between the wall and the gauge. These gauges are then connected to a data logger (AOIP Instruments SAM-70) whose acquisition is every 3 s. From bottom to top, these thermocouples were stuck at the respective locations 2 mm, 5 mm, 10 mm, 20 mm, 35 mm, 60 mm, 90 mm, 130 mm and 180 mm. Derived from the integral method analysis [22], the experimental measurement of the surface temperatures leads to the determination of the experimental heat flux delivered to water from the analytical formula (1) giving the temperature gradient at wall in free boundary layer convection, so that

$$\left(T_w - T_\infty\right) = \left[\frac{27\varphi_w^4 \nu^2 \Delta^4 \left(9\Delta - 5\right)}{2g\beta k^4} y\right]^{1/5} \qquad (1)$$

where $\Delta = \delta_T / \delta$ is the thermal to hydrodynamical boundary layer thickness ratio estimated from the von Karman–Pohlhausen integral method extended to the general case with no assumption of a common boundary layer thickness for both thermal and velocity [23]. Δ is numerically calculated by solving the deduced governing equations of steady free convection on vertical heated surfaces and assumed to be no-time dependent [24]. Δ is numerically found to be 0.653 for Pr = 7. The superposing of the experimental and analytical (eq. 1) curves allows then to go back easily to the heat flux which is transmitted to the fluid.

As an example, Figure 2 illustrates the spatial evolution of the temperature gradient at wall, from both experiments and analytical point of view. A very good agreement between curves is found for a heat flux equal to φ_w = 445 W/m². Moreover, to complete the analysis about the early stages in the development of the dynamics of such open-ended channel flow, a 1550 W/m² uniform heat flux has also been considered. Corresponding modified Rayleigh numbers are presented in Table 1.

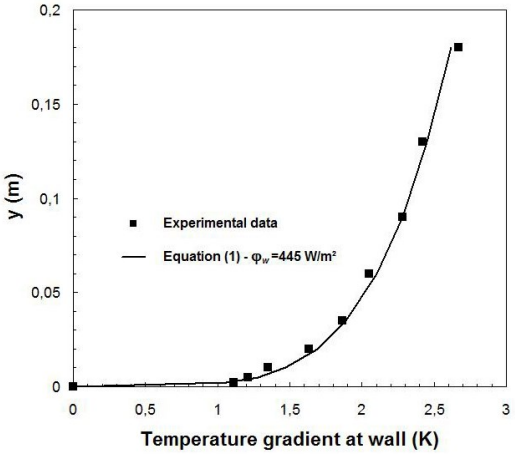

Figure 2 Experimental and analytical temperature profiles for φ_w = 445 W/m²

Table 1 Range of Rayleigh numbers

Heat flux (W/m²)	Modified Rayleigh Ra*
445	$2.2\ 10^6$
1550	$7.6\ 10^6$

No-stratification verification

Experiments have been carried out 30 min after the tank was filled with water in order to consider the fluid at rest and to ensure a quasi-uniform tank temperature. Nevertheless because of the difference that exists between the fluid temperature inside the tank and the room temperature, a buoyancy driven flow along the tank side walls occurs. This parasitic flow leads to a thermal stratification phenomenon which was measured using nine thermocouples evenly spaced along a vertical axis within the tank. A 0.5 °C/m thermal stratification has been measured from stratification profiles that have been found to present no evolution during the first 5 minutes following the initiation of the heating device. In such a way, this weak stratification has been assumed to have no influence on the dynamics of the convective flow in the channel.

Velocity uncertainties

The dynamical analysis mainly interests streamline patterns and velocity profiles which are based upon the particle paths. Of course the particles are not neutrally buoyant so that they have a sedimentation velocity. It is advisable to quantify this sedimentation velocity [25] to see how it can influence the particle trajectories.

Applying Stokes' law (eq. 2) for a 10 μm average particle diameter leads to a sedimentation velocity $V_s = 2.21\,\mu\text{m.s}^{-1}$ which can be neglected with regard to velocities within the channel even if in the early transient, the velocities are very low within the dynamical boundary layer and later within the whole channel.

$$V_s = \frac{g d_p^2}{18\nu_f}\left(\frac{\rho_p}{\rho_f} - 1\right) \qquad (2)$$

DISCUSSION

In a geometrical configuration where the environment would be considered as semi-infinite (corresponding to an aspect ratio $R_f \rightarrow 0$), the boundary layer which develops along a heated wall thickens as it is fed by fluid coming from the crosswise direction from the wall. Figure 3 illustrates this fact from a theoretical viewpoint [25] in the case of a vertical plate initially located in a quiescent fluid and impulsively submitted to a uniform heat flux thermal condition.

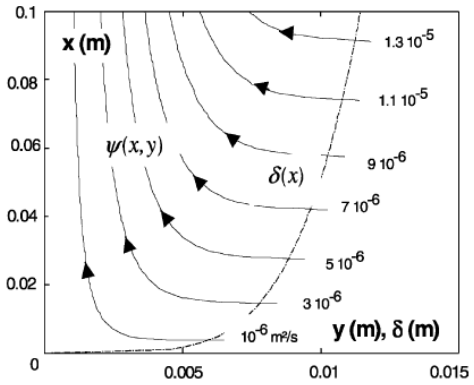

Figure 3 Theoretical streamline patterns [25] for $R_f \rightarrow 0$ and $\varphi_w = 100$ W/m²

Transient and steady-state flow dynamics

In the case of an open-ended channel, the lateral feeding of the boundary layer is then impeded by the effect of the channel confinement. It is this peculiar feeding phenomenon of the viscous layer which, during the very first instants, is going to cause the appearance of large-scale flow instabilities which are going to evolve and propagate until a return flow develops.

The steady-state regime of the natural convection flow in the channel was investigated in a previous study [2]. Three modified Rayleigh numbers ($4.3\text{x}10^5 < \text{Ra}^* < 4.5\text{x}10^6$) as well as three aspect ratios (R_f = 5.2; 6; 6.9) were studied. The steady-state regime was observed to occur after about thirty minutes of heating. In all studied cases, an upward boundary layer flow was found near the heated wall, accompanied by a reverse flow developing on the opposite side from the top-end of the channel, the reverse flow taking the form of an elongated eight-shaped structure with two main recirculation cells. In order to provide a more detailed analysis of the mechanism leading to the steady-state flow structure, streamline patterns showing two intermediate structures obtained during the transient (at $t = 10$ min and $t = 20$ min after the start of the heating) as well as one in steady state regime (at $t = 50$ min) are plotted in Figure 4. Streamline patterns were deduced from visualizations of the water flow field by using laser tomography and small solid particles as discrete tracers (See Ospir et al. [2] for more details). As similar patterns were observed in the range of aspect ratios and modified Rayleigh numbers investigated, streamline patterns are only provided for one case, i.e. R_f=5.2 ($b = 36$ mm) and $\text{Ra}^*=4.5\times10^6$. Figure 4a shows a large single recirculation cell that developed during the transitional phase corresponding to the first moments of heating. This recirculation cell appears only a few minutes after the start of the heating and extends over most of the channel width. Then, a second cell is progressively forming, as illustrated by Figure 4b, in order to finally give the eight-shaped structure consisting of two cells observed in Figure 4c. The bifurcation observed from the streamline patterns in Figure 4 is due to the presence of a separation point at the cold wall (right wall in Figure 4) and separation line (not drawn in Figure 4) occurring in counter-courant flow situations at wall. At the cold wall, the main flow from bottom to top encounters the primary vortex penetrating the open channel from the top. The principal influence on the viscous flow between the main primary vortex and the right cold wall is the induced adverse pressure gradient impressed to the bottom of the primary vortex shown with the distortion of the streamlines (see Figure 4b; t=20 min). Consequently, the compression of the vorticity field near the bottom of the primary vortex leads to "break" this primary vortex to create a secondary co-rotating vortex. The characteristics of the upper cell are similar to that of the initial single cell of the transitional phase, except for its reduced length. As concerns the lower cell, it is located at the bottom of the zone previously occupied by the initial cell and extends a bit further down the channel.

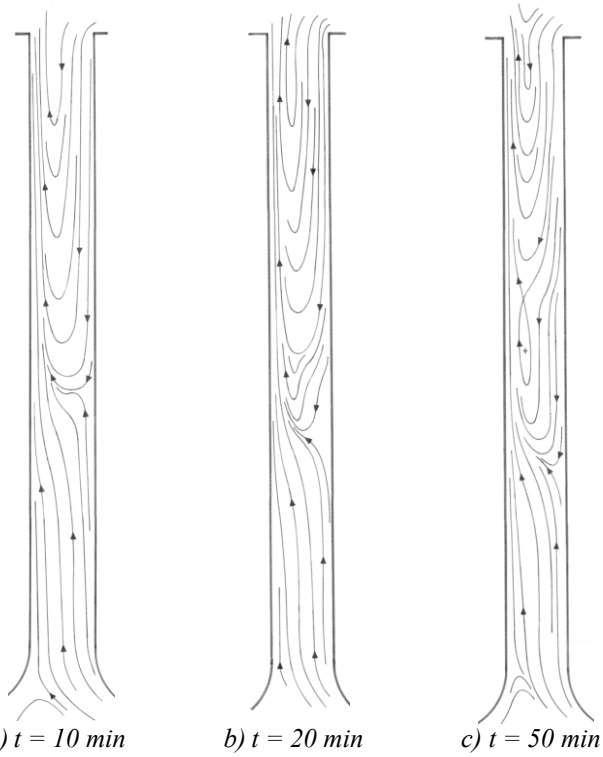

Figure 4 Streamline patterns during the transient (t= 10 min and $t = 20$ min) and in steady-state regime ($t = 50$ min) for $\text{Ra}^*=4.5\times10^6$ and R_f=5.2 (From Ospir et al. [2])

Early-transient streamline patterns

In order to better understand the process of formation of the dynamic structures of the flow, the current study deals more specifically with the very first moments that led to the transient

dynamic structure observed in Figure 4a. Thus, Figures 5 and 6 focus on temporal sequences of streamline patterns showing the development and time-evolution of these flow instabilities, deduced from PIV experiments.

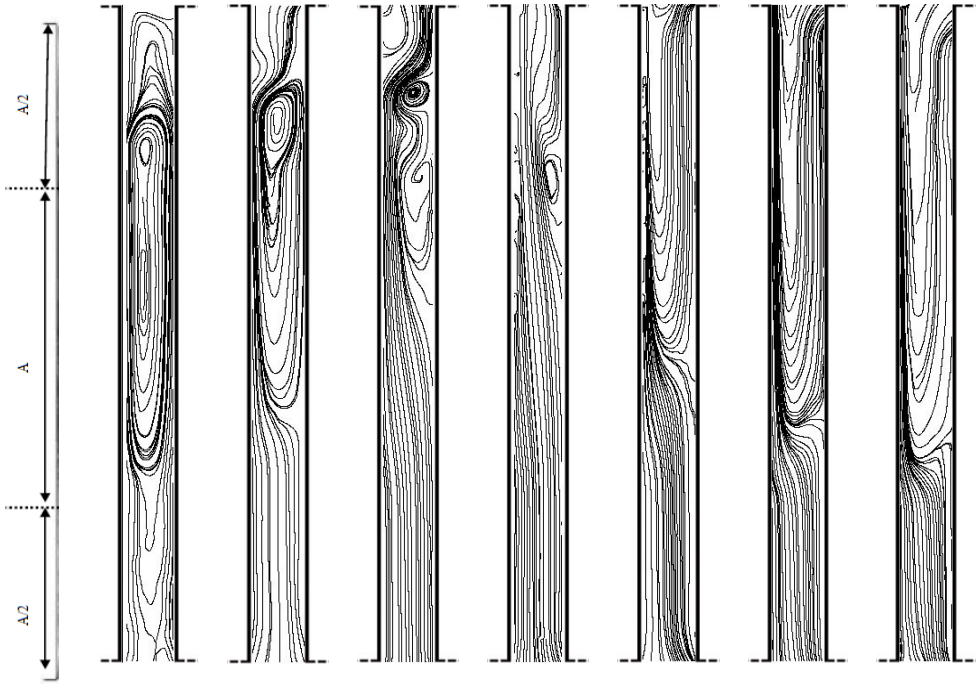

Figure 5 Streamline patterns for 445W/m² (t=60-90-120-180-240-270-300s)

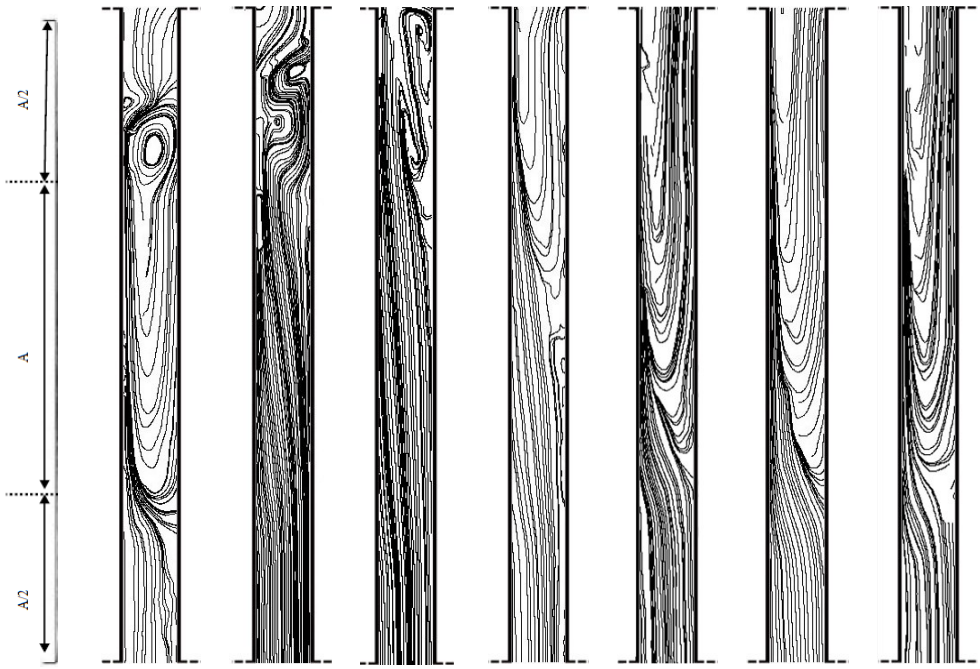

Figure 6 Streamline patterns for 1550 W/m² (t=60-90-120-180-240-270-300s)

In Figure 5, corresponding to a 445 W/m² heat flux, the early stages ($t < 60$ s) are materialized by a primary large-scale vortex whose initial main dimension is that of the heated zone. This primary vortex is clock-wise, presents a core in its top and induces a weak secondary counter-clock wise vortex ($t = 90$ s) attached to the left wall. These primary and secondary vortices form a counter rotating vortex couple whose interaction results in an upward motion of the viscous layer from the heated left wall. The more the secondary vortex enlarges, the more the boundary layer separates from the heated wall to reach a location close to the adiabatic wall. Increasing time leads to the shedding of the secondary vortex out of the channel exit. At $t = 120$ s, the primary eddy attached to the adiabatic wall exhibits a vortex splitting phenomenon into two co-rotating

cells forming an eight-shape vortex. The swelling of the upper cell and its ascending motion have for consequence to tip over the boundary layer towards the left side. It seems that this transverse beating of the separated boundary layer combined with the presence of the attached lower cell ($t = 180$ s) is responsible for the appearance of a major return flow ($t > 180$ s) by originating an imbalance of the pressure field at the channel outlet

This strong reversal flow occupies the major part of the channel and its penetration length reaches, in the studied time range up to 300 s, the location of the beginning of the heating process.

To confirm the observed trends, Figure 6 presents the time-evolution of the streamline pattern maps for a heat flux value of 1550 W/m² corresponding to a modified Rayleigh number $Ra^* = 7.6 \times 10^6$. In general, one finds exactly the same vertical instabilities as the previous thermal condition case, namely the development of a couple of primary and secondary vortices, the phenomenon of vortex splitting of the primary cell attached to the adiabatic wall, the vortex shedding process out of the channel exit, as well as the oscillation or beating of the viscous layer. What differs is the time of appearance of these phenomena, noticed faster for a higher value of the heat flux.

Evidence of a mushroom-like vortex

The role of the secondary cell attached to the heated wall seems essential in the birth of instabilities in the confined flow within the channel. It is indeed this eddy which is going to make the warm fluid layer tip over towards the adiabatic wall. In order to better understand how the secondary vortex develops, a streakline complementary analysis from laser tomography method (Figure 7) has been led in the vicinity of the heated wall. It clearly appears that the distortion of the warm fluid layer rolling-up creates an instability. This instability generates itself an opposite rolling-up due to the blocking effect occurring when the hot fluid in its ascending motion encounters colder fluid of higher density. It is noticed that the resulting couple of primary and secondary vortices acts like a mushroom-like vortex of asymmetrical shape due to the close presence of the left heated wall.

Topological synthesis

As already mentioned, the early stages in the development of the free convection flow within the open-ended channel asymmetrically heated are subject to numerous vortical instabilities. In a simplistic way, one can summarize the development of the free convection flow at four consecutive and different stages leading to the establishment of the large-scale reversal flow in the open-ended channel, as shown in the synopsis of Figure 8.

1/ Creation from the start of the heating of a primary cell C1, due to fluid feeding of the hot boundary layer in confined domain.

2/ Hot viscous layer separation from left to right due to the swelling of a secondary cell C2 attached to the left wall.

3/ Vortex splitting of the primary C1 cell in two co-rotating cells C1 and C3.

4/ Upward convection motion of C1 leading to the shedding of C2 and consecutively to the viscous layer beating from right to left. As a result, the extension of C3 occurs giving way to the appearance of a major reversal flow.

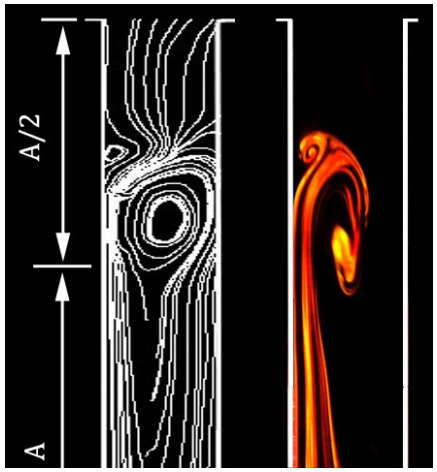

Figure 7 Streamline patterns from PIV (left) – Corresponding streaklines from sulforhodamine dye visualization (right) at t = 60 s for a 1550 W/m² heat flux

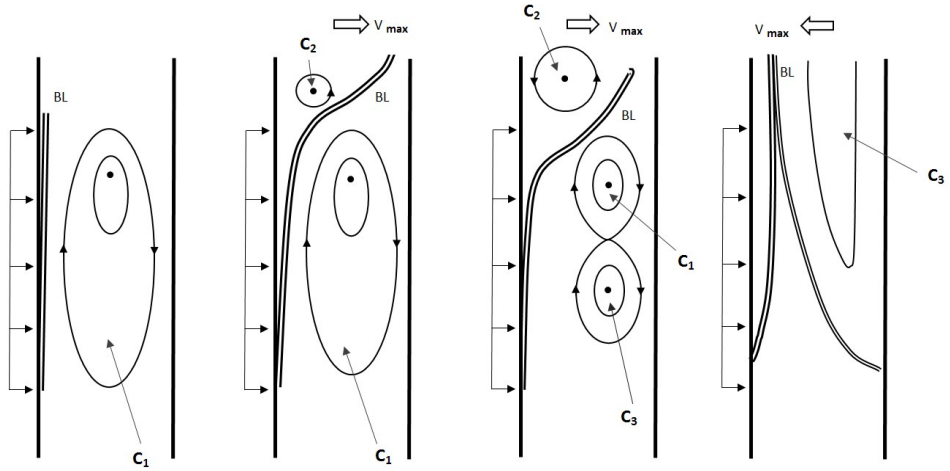

Figure 8 Synoptic of the topological sequences

Velocity profiles

To complete the phenomenological observation of hydrodynamic instabilities developing within the channel, both inlet and outlet velocity profiles deduced from PIV experiments have been drawn in Figures 9 and 10. Three different moments were held for every studied heat flux thermal boundary condition. In Figure 9 for a 445 W/m² UHF condition, the inlet velocity profiles show a relatively regular behaviour except in the area close the left and right solid boundaries. The reason is that an asymmetrically heated channel ineluctably leads to an asymmetrically upstream feeding flow of slightly oblique shape. The maximum velocity value in the middle axis of the channel is about 1.8 mm/s at $t = 180$ s. The outlet velocity profiles clearly exhibit the beating phenomenon of the hot boundary layer. Indeed, increasing time shows how the velocity peaks alternately go from the right to the left channel walls. One notices that at the chosen times, the outlet velocity values are positive, realizing the absence of whirling structures inducing secondary reverse flows.

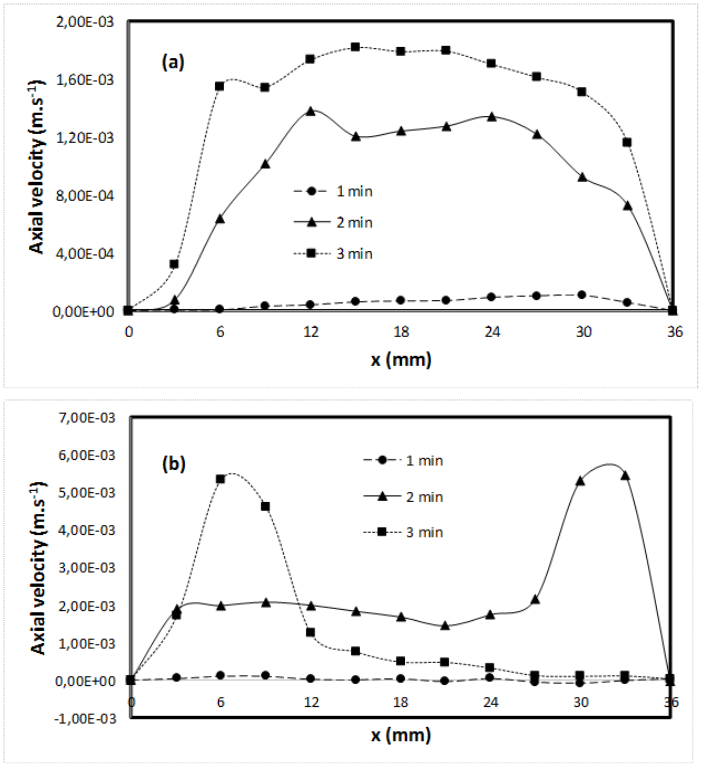

Figure 9 Axial velocity for 445 W/m²
(a) channel inlet (b) channel outlet

Looking at Figure 10 and focusing on the channel inlet, one can see the axial velocity profiles in the central region of the section $-b/4 < y < +b/4$ presenting a flat shape, with a nearly uniform value. This value increases with increasing time. At the channel outlet, the velocity profiles highlight the beating phenomenon of the hot boundary and these profiles show negative values. This fact indicates that, at these given times, the fluid moves inside the channel downwards, producing a circulation zone.

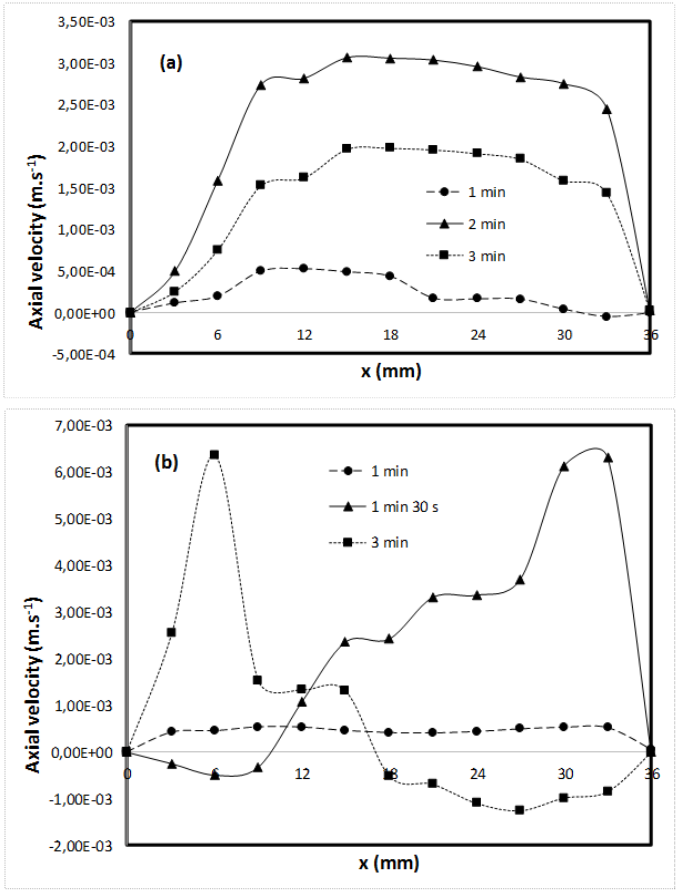

Figure 10 Axial velocity for 1550 W/m²
(a) channel inlet (b) channel outlet

CONCLUSION

The experimental investigation carried out in this article showed the fluid dynamics during the early stage regime of free convection in water inside a vertical channel asymmetrically heated at uniform heat flux. The problem is assumed to be two-dimensional and the analysis is made in the middle-section of the channel for a modified Rayleigh number ranging from 2.2×10^6 to 7.6×10^6. Deduced from Particle Image Velocimetry (PIV), the analysis allowed to detect a complex topological behaviour in the internal flow leading to numerous instabilities whose topological features are described. Vortex formation and shedding, vortex splitting, separation and beating of the boundary layer from one wall to another are identified, leading to an imbalance in the outlet pressure field which is certainly at the origin of a large-scale reversal flow. A mushroom-like vortex formation is also observed. Axial velocity profiles are also established, confirming the structural observations. The different events appear whatever the heat flux density is, namely 445 W/m² or 1550 W/m². What differs is the appearance time of the phenomena, observed to be faster for a higher heat flux.

ACKNOWLEDGMENTS

This study has been supported by the French Research Group GDR AMETh: Analyse – Maîtrise des Ecoulements et Echanges Thermiques.

REFERENCES

[1] Desrayaud G., Chénier E., Joulin A., Bastide A., Brangeon B., Caltagirone J.P., Chérif Y., Eymard R., Garnier C., Giroux-Julien S., Harnane Y., Joubert P., Laaroussi N., Lassue S., Le Quéré P., Li R., Saury D., Sergent A., Xin S., and Zoubir A., Benchmark solutions for natural convection flows in vertical channels submitted to different open boundary solutions, *International Journal of Thermal Sciences*, Vol. 72, 2013, pp. 18-33

[2] Ospir D., Popa C., Chereches C., Polidori G., and Fohanno S., Flow visualization of natural convection in a vertical channel with asymmetric heating, *International Communications in Heat and Mass Transfer,* Vol. 39, 2012, pp. 486–493

[3] Gan G., A parametric study of Trombe walls for passive cooling of buildings, *Energy and Buildings,* Vol. 27, 1998, pp. 37-43

[4] Ding W., Hasemi Y., and Yamada T., Natural ventilation performance of a double-skin façade with a solar chimney, *Energy and Buildings,* Vol. 37, 2005, pp. 411-418

[5] Fossa M., Ménézo C., and Leonardi E., Experimental natural convection on vertical surfaces for building integrated photovoltaic (BIPV) applications, *Experimental Thermal and Fluid Science*, Vol. 32, 2008, pp. 980-990

[6] Elenbaas W., Heat dissipation of parallel plates by free convection, *Physica*, Vol. 9, 1942, pp. 1-28

[7] Sparrow E.M., and Azevedo L.F.A., Vertical-channel natural convection spanning between the fully-developed limit and the single-plate boundary-layer limit, *International Journal of Heat and Mass Transfer*, Vol. 28, 1985, pp. 1847-1857

[8] Wirtz R.A., and Stutzman R.J., Experiments on free convection between vertical parallel plates with symmetric heating, *ASME Journal of Heat Transfer*, Vol. 104, 1982, pp. 501-507

[9] Webb B.W., and Hill D.P., High Rayleigh number laminar natural convection in an asymmetrical heated vertical channel, *ASME Journal of Heat Transfer*, Vol. 111, 1989, pp. 649-656

[10] Dupont F., Ternat F., Samot S., and Blonbou R., Two-dimension experimental study of the reverse flow in a free convection channel with active walls differentially heated, *Experimental Thermal and Fluid Science*, Vol. 47, 2013, pp. 150-157

[11] Daverat C., Etude expérimentale de la convection naturelle en canal vertical à flux de chaleur imposé – application au rafraîchissement passif de composants actifs de l'enveloppe des bâtiments, *PhD Thesis*, INSA Lyon, France, 2012

[12] Daverat C., Pabiou H., Ménézo C., Bouia H., and Xin S., Experimental investigation of turbulent natural convection in a vertical water channel with symmetric heating : Flow and Heat Transfer, *Experimental Thermal and Fluid Science*, Vol. 44, 2013, pp. 182-193

[13] Habib M.A., Said S.A.M., Ahmed S.A., and Asghar A., Velocity characteristics of turbulent natural convection in symmetrically ans asymmetrically heated vertical channels, *Experimental Thermal and Fluid Science*, Vol. 26, 2002, pp. 77-87

[14] Zoubir A., Daverat C., Xin S., Giroux-Julien S., Pabiou H., and Ménézo C., Natural convection in a vertical open-ended channel : comparison between experimental and numerical results, *Journal Energy and Power Engineering*, Vol. 7, 2013, pp. 1265-1276

[15] Yilmaz T., and Gilchrist A., Temperature and velocity field characteristics of turbulent natural convection in a vertical parallel plate channel with asymmetric heating, *Heat and Mass Transfer,* Vol. 43, 2007, pp. 707-719

[16] Sanvicente E., Giroux-Julien S., Ménézo C., and Bouia H., Transitional natural convection flow and heat transfer in an open channel, *International Journal of Thermal Sciences*, Vol. 63, 2013, pp. 87-104

[17] Sparrow E.M., Chrysler G.M., and Azevedo L.F., Observed flow reversals and measured-predicted Nusselt numbers for natural convection in a one-sided heated vertical channel, *ASME Journal of Heat Transfer*, Vol. 106, 1984, pp. 325-332

[18] Andreozzi A., Buonomo B., and Manca O., Numerical study of transient natural convection in vertical asymmetrically heated channels, *Proceedings of the 61st Congresso Nazionale ATI*, Perugia, Italy, September 2006 (6 pages)

[19] Li R., Bousetta M., Chénier E., and Lauriat G., Effect of surface radiation on natural convective flows and onset of flow reversal in asymmetrically heated vertical channels, *International Journal of Thermal Sciences*, Vol. 65, 2013, pp. 9-27

[20] Cao X., Liu J., Jiang N., and Chen Q., Particle image velocimetry measurement of indoor airflow field: A review of the technologies and applications, *Energy and Buildings,* Vol. 69, 2014, pp. 367-380

[21] Polidori G., and Padet J., Transient free convection flow on a vertical surface with an array of large-scale roughness elements. *Experimental Thermal and Fluid Science*, Vol. 27, 2003, pp. 251–260

[22] Padet J., Principes des Transferts Convectifs, Polytechnica ed, Paris, 1997.

[23] Polidori G., Mladin E.C., and de Lorenzo T., Extension de la méthode de Karman–Pohlhausen aux régimes transitoires de convection libre, pour Pr > 0,6, *Comptes Rendus de l'Académie des Sciences – Serie IIb : Mécanique,* Vol. 328, 2000, pp. 763–766

[24] Fohanno S., and Polidori G., Effect of the gap size in the start-up free convective flow around a square prism near a wall. *International Journal of Heat and Fluid Flow,* Vol. 26, 2005, pp. 25–33

[25] Polidori G., Popa C.V., and Mai T.H., Transient flow rate behaviour in an external natural convection boundary layer, *Mechanics Research Communications,* Vol. 30, 2003, pp. 615-621